Radical-scavenging and UV-radiation absorption activities of aaptamine derivatives: DFT and TD-DFT studies

Doan Thi Hoai Nam[1], Thi Le Anh Nguyen[2,3,*], Nguyen Thi Ai Nhung[4], Duong Tuan Quang[5], Duy Quang Dao[2]

[1]*Department of Chemistry, Danang University of Science and Technology - The University of Danang, Da Nang, 550000, Vietnam*

[2]*Institute of Research and Development, Duy Tan University, Da Nang, 550000, Vietnam*

[3]*Faculty of Natural Sciences, Duy Tan University, Da Nang, 550000, Vietnam*

[4]*Department of Chemistry, University of Sciences, Hue University, Hue city, 530000, Vietnam*

[5]*Department of Chemistry, University of Education, Hue University, Hue city, 530000, Vietnam*

Received: xxx; Accepted for Publication: xxx

Abstract

Antioxidant and UV absorption activities of three aaptamine derivatives including piperidine[3,2-b]demethyl(oxy)aaptamine (**C1**), 9-amino-2-ethoxy-8-methoxy-3H-benzo[de][1,6]naphthyridine-3-one (**C2**), and 2-(sec-butyl)-7,8-dimethoxybenzo[de]imidazo[4,5,1-ij][1,6]-naphthyridin-10(9H)-one (**C3**) were theoretically studied by density functional theory (DFT). Optimized geometries of **C1**–**C3** and theirs intrinsic thermochemical properties such as bond dissociation energy, proton affinity, and ionization potential were calculated at DFT/M05-2X/6-311++G(d,p) level of theory *in vacuo* and in water. The results show that **C1–C3** exhibited similar potent antioxidant activities, which are comparable to well-known antioxidants such as Trolox or cembrene. The radical scavenging activity of the antioxidants were then investigated by evaluation the Gibbs free energy ($\Delta_r G^0$) of the reaction between **C1**–**C3** and the $HOO^{\bullet}/HO^{\bullet}$ radicals *via* four mechanisms, including: hydrogen atom transfer (HAT), single electron transfer (SET), proton loss (PL) and radical adduct formation (RAF). Kinetic calculation reveals that $HOO^{\bullet}$ scavenging in water is occurred *via* HAT mechanism with **C1**@C19 while RAF is more dominant with **C2** and **C3**. Antioxidant activity of aaptamine derivatives can be classified as **C1** > **C3** > **C2**. In addition, all compounds are active in UV-Vis absorption; the excitations of which are determined as π-π* transition. Overall, the results suggest the potential applications of the aaptamines in pharmaceutics and cosmetics, *i.e.* as sunscreen and antioxidant ingredient.

Keyword: *Aaptamine, TD-DFT, antioxidant, free radical scavenging, UV-filter*

1. INTRODUCTION

Aaptamines are commonly known marine natural products, which have been extracted from *Aaptos aaptos* species in the marine milieu of the Pacific ocean, *i.e.* Malaysia,[1] Vietnam,[2] and Indonesia.[3] The first aaptamine structures, extracted from a Japanese sponge and characterized by Nakamura *et al.*,[4] are identified as alkaloid-based compounds containing the 1H-benzo[de]-1,6-naphthyridine skeleton. To date, there is a large number of research which reported different biological activities of aaptamines such as antifungal,[2 5] antiviral,[6] antimicrobial,[7] and anticancer.[1 3 8 9 10] In particular, antioxidant activity of aaptamines was early predicted and studied. Indeed, aaptamines and isoaaptamine, amongs other marine sponges, were reported for strong antioxidant activity against DPPH radical.[11] In a perspective view, besides the natural and well-disposed origin, the antioxidant properties as well as other biological activities of the aaptamines can be of human-health-benefit because that helps protect our body from free radicals, fight aging, boosting the immune system, and prevent diseases.

On the other hand, oxidative stress (OS) resulting from long-time ultraviolet radiation (UVR) exposure is identified as one of the main causes for skin aging, DNA skin damage and melanogenesis.[12] At the early stage of the sunscreen research started by the 1940s, most of the products targeted minimizing the effect of UVB (280–315 nm) radiation because the direct UVB absorption by DNA generates UV-signature mutations leading to DNA lesions and carcinogenic effect.[13] Scientists later discovered that the UVA (315–400 nm) can deeply penetrate into the skin, producing reactive oxygen species (ROS) and reactive nitrogen species (RNS) in human skin that cause DNA and other biological molecules to be damaged and so is not less harmful than the UVB to human skin.[14 15] One of the common mechanism, for example, is the ROS-mediated cell damage by peroxidation of fatty acids within the phospholipid structure of the membrane. Today, a broad-spectrum UV filter that covers both UVA and UVB is one of the most

important properties for candidate compounds potentially applied in organic sunscreen.[16]

Moreover, the photo-protective properties of natural products have been earlier reported for natural antioxidants including polyphenols,[17] stilbenes,[18] hydroxycinamate derivatives.[19] [20] A large number of studies have shown positive effect of antioxidant in the skin, for both treatment and prevention of inflammation, oxidation, sebaceous glands or melanogenesis.[21] Multiple mechanisms of skin photo-protective have also been documented.[15] In addition, the synthesis of p-hydroxycinnamic diacids such as of ferulic, sinapic, p-coumaric and caffeic diacid, the resulting molecules show potent antioxidant and UV filter.[22] Recently, we reported the antioxidant and photo-protective properties of different natural compounds in which the cycloechinulin and wasabidienone extracted from marine fungus showed the most potential antioxidant and photo-protective properties.[23] To the best of our knowledge, there have not been any studies that consider both the radical scavenging and photo-protective properties of the aaptamine derivatives.

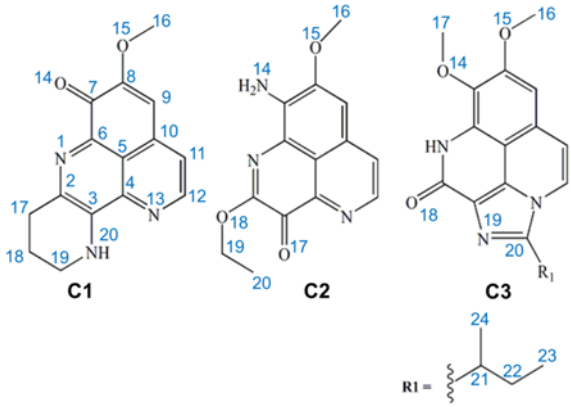

Figure 1. Chemical structure of **C1-C3**.

In this study, the antioxidant properties through free radical scavenging activity and the UV filter properties of three different aaptamine derivatives including piperidine[3,2-b]demethyl(oxy)aaptamine (**C1**), 9-amino-2-ethoxy-8-methoxy-3H-benzo[de][1,6]naphthyridine-3-one (**C2**), and 2-(sec-butyl)-7,8-dimethoxybenzo[de]imidazo[4,5,1-ij][1,6]-naphthyridin-10(9H)-one (**C3**) reported by Nakamura *et al.* (Figure 1) were elucidated using density functional theory (DFT). Thermodynamic parameters of reaction characterized the antioxidant activity of three aaptamines **C1–C3** *via* four common mechanisms: hydrogen atom transfer (HAT), single electron transfer (SET), proton loss (PL), and radical adduct formation (RAF) were focused. Different intrinsic thermochemical parameters including bond dissociation enthalpy (BDE), adiabatic ionization potential (IP) and proton affinity (PA) were calculated at the gas phase (*vacuo*) and water. The reaction enthalpies ($\Delta_r H^0$) and standard Gibb free energies ($\Delta_r G^0$) of four reactions between the studied compounds and $HOO^\bullet$, $OH^\bullet$ radicals were also examined to elucidate their scavenging capabilities. Finally, the time-dependent density functional theory (TD-DFT) was used to elucidate the UV-Vis absorption mechanism of the three aaptamines.

2. COMPUTATIONAL METHOD

Gaussian 16 revision A.03 package was used to optimize the geometrical and electronic structures of the studied compounds.[24] All calculations were performed at the DFT/M05-2X/6-311++G(d,p) level of theory.[25] The M05-2X is previously reported to have a good benefit for the TS location and kinetics calculation. [26] [27]

The four main working mechanisms, including hydrogen atom transfer (HAT), single electron transfer (SET), proton loss (PL) and radical adduct formation (RAF) have been investigated.

In the first approach, the intrinsic thermochemical parameters characterizing for three mechanisms HAT, SET, and PL were calculated according to the following reaction equations:

+ Hydrogen atom transfer (HAT):

$A–H \rightarrow A^\bullet + H^\bullet$ (BDE); (R1)

+ Single electron transfer (SET):

$A–H \rightarrow AH^{+\bullet} + e^-$ (IP); (R2)

+ Proton transfer (PT):

$A–H \rightarrow A^- + H^+$ (PA); (R3)

Based on the equations R1-R3, intrinsic thermodynamic parameters such as bond dissociation enthalpies (BDE), adiabatic ionization potential (IP), and proton affinities (PA) were calculated as follows:

$BDE\ (A–H) = H(A^\bullet) + H(H^\bullet) – H(A–H)$; (eq.1)

$IP\ (A–H) = H(AH^{\bullet+}) + H(e^-) – H(A–H)$; (eq.2)

$PA\ (A–H) = H(A^-) + H(H^+) – H(A–H)$; (eq.3)

in which, H accounts for the total energy of the studied species at 298.15K and 1 atm. The experimental energy value of the proton (H^+) and the electron (e^-) in gas phase was 1.4811 and 0.7519 kcal.mol^{-1}, respectively.[28] In water, the energy values of the proton $H(H^+)$ and of electron $H(e^-)$ were -235.3 and -23.9 kcal.mol^{-1}, respectively; calculation method was previously reported. [29]

In order to evaluate the influence of chemical nature of free radicals on the antioxidant potential of the studied compounds *vs.* representative radicals such as $HOO^\bullet$, the standard Gibbs free energies of the reaction ($\Delta_r G^0$) were calculated for HAT, PL, RAF and SET mechanisms according to the R4–R7 reactions (eq.4–eq.7). Similar results for the $HO^\bullet$ radical scavenging reactions were obtained in

replacing the corresponding values of $HOO^{\bullet}$ by that of $HO^{\bullet}$ radical.

HAT: A–H + $HOO^{\bullet} \rightarrow A^{\bullet}$ + HOOH; (R4)

PL: A–H + $HOO^{\bullet} \rightarrow A^{-}$ + $HOOH^{\bullet+}$; (R5)

RAF: A–H + $HOO^{\bullet} \rightarrow$ AH–$OOH^{\bullet}$; (R6)

SET: A–H + $HOO^{\bullet} \rightarrow AH^{\bullet+}$ + HOO^{-}; (R7)

Standard Gibbs free energies ($\Delta_r G^0$) of the reactions were calculated as follows:

$\Delta_r G^0$ (HAT) = [$G(A^{\bullet})$ + G(HOOH)] – [G(A–H) + $G(HOO^{\bullet})$]; (eq.4)

$\Delta_r G^0$ (PL) = [$G(A^{-})$ + $G(HOOH^{\bullet+})$] – [G(A–H) + $G(HOO^{\bullet})$]; (eq.5)

$\Delta_r G^0$ (RAF) = G(AH–$OOH^{\bullet}$) – G(A–H) – $G(HOO^{\bullet})$; (eq.6)

$\Delta_r G^0$ (SET) = [$G(AH^{\bullet+})$ + $G(HOO^{-})$] – [$G(HOO^{\bullet})$ + G(A–H)]; (eq.7)

The kinetics of HT and RAF reactions in the gas phase and the water were studied in this work based on quantum mechanics-based test for overall free radical scavenging activity (QM-ORSA) protocol[26] using the Eyringpy code.[30] Details of this calculation can be found in our previous work.[23]

$$k(T) = \sigma\kappa \frac{k_B T}{h} e^{\frac{-\Delta G^{\ddagger}}{RT}} \quad \text{(eq.8)}$$

Where $\Delta G^{\ddagger}$ is the Gibbs free energy of activation; T is the temperature in Kelvin; k_B is the Boltzmann constant and h is the Planck constant; σ is the reaction symmetry number (or the reaction path degeneracy), κ is the transmission coefficient attributing for the quantum tunneling effects by employing Eckart barrier. The solvent cage effect was included according to the correction proposed by Okuno,[31] taking into account the free volume theory.[32]

For SET reaction, the Marcus theory[33] was applied for the estimation of the electron transfer rate. The energy barrier was obtained as eq. 9.

$$\Delta G_{SET}^{\ddagger} = \frac{\lambda}{4}\left(1 + \frac{\Delta G_{SET}^{0}}{\lambda}\right)^2 \quad \text{(eq.9)}$$

Where ΔG^0_{SET} is the free energy of reaction; λ is the nuclear reorganization energy which can be calculated by the difference of ΔE_{SET} and ΔE^0_{SET}, with ΔE_{SET} is the vertical energy between reactants and products of the reaction *via* SET mechanism.

In solvent, diffusion rate k_D may be important and greatly contributes to the apparent rate constant k_{app}. Therefore, the Collins-Kimball theory[34] was employed (eq.10).

$k_{app} = k_D.k/(k_D+k)$ (eq.10)

Where k is the thermal rate constant and k_D is the diffusion rate constant calculated follow Smoluchowski[35] (eq.11).

$k_D = 4\,\pi\, R_{AB} D_{AB} N_A$ (eq.11)

where the R_{AB} is the reactant distance, D_{AB} is the mutual diffusion coefficient of the antioxidant A and radical B ($HOO^{\bullet}$); D_{AB} is resulting from the Stockes-Einstein approach[36 36b] (eq.12)

$D_{AB} = k_B.T/(6\pi\eta r)$ (eq.12)

In which k_B is the Boltzmann constant, T is temperature and η is the viscosity of the solvent (8.91×10^{-4} P.s) and r is the radius of the solute.

For the basidity of the aaptamines, the pK_a calculation was performed following the thermodynamic cycle previously reported.[37 38]

pK_a of the **C1**-**C3** were determined as (eq.13)

$pK_a = \Delta G^0_{deprot,aq}/RTln(10)$ (eq.13)

in which the $\Delta G^0_{deprot,aq}$ is the solution-phase standard free energy of deprotonation which can be calculated by thermodynamic cycle.

The vertical excitation of **C1**–**C3** in methanol was calculated using TD-DFT approach. A small benchmark of functionals with different exchange correlation XC part, *i.e.* B3LYP, B98, M06, PBE0, CAMB3LYP, and M05-2X were employed with the same basis set as the previous part. These functionals are chosen following the recommendation by Jacquemine *et al.* for low Mean signed Error (MSE) and Mean absolute Error (MAE) for singlet excited states.[39] Solvent effects were implicitly studied using the Polarization Continuum Model (IEF-PCM).[40]

3. RESULTS AND DISCUSSION

3.1. Structure and electronic properties

The optimized structures and electronic properties of the three studied aaptamine compounds calculated by DFT method at M05-2X/6-311++G(d,p) level of theory in the gas phase are shown in Figure 2.

As can be seen in Figure 2, compounds **C1**-**C3** share the benzo[de][1,6]naphthyridine skeleton and similarly have $–OCH_3$ group attached to C8 position. At C7, the substituent groups such as ketone (=O), amine ($–NH_2$) and methoxy ($–OCH_3$) are attached to the B ring, in **C1**, **C2** and **C3**, respectively. The main difference in the chemical nature of three compounds is the substituent groups found at the A ring, for **C1** a N-containing six-membered cycle, for **C2** the =O and $–OC_2H_5$ group, and for **C3** a N-containing five-membered cycle with 2-butyl derivative that is shared both A and C ring. Moreover, the electronic distribution on the frontier molecular orbitals such as the highest occupied molecular orbital (HOMO) and the lowest

unoccupied molecular orbital (LUMO) shows that all the rings play a key role in electron-donating (HOMO distribution) and electron-accepting (LUMO distribution) reactions with free radicals. For all molecules, the electrostatic potential (ESP) maps display a negative region on the C=O groups and the nearby carbons.

3.2. Basidity

The pK_a of three aaptamines **C1-C3** calculated at M05-2X/6-311++G(d,p) level of theory is presented in Table 1. Similar calculation for aniline at the same level of theory was performed for comparison; the obtained value of pK_a is 31.1 for aniline, consistent with the experimental data, *i.e.* 30.6, reported in DMSO and 28 in water. [41] [42] For our aaptamines, the result shows that pK_a of **C1-C3** are of about 22-23. Therefore, in the following calculation we can consider the neutral form of **C1-C3** in water.

Table 1. pK_a of **C1-C3** calculated in water at the M05-2X/6-311++G(d,p) level of theory

Cpd	**C1**	**C2**	**C3**	**Aniline**
pK_a	22.79	23.57	22.42	31.11*

*Exp. value of 30.6 in DMSO and 28 in water (Bordwell 1977, 1988)

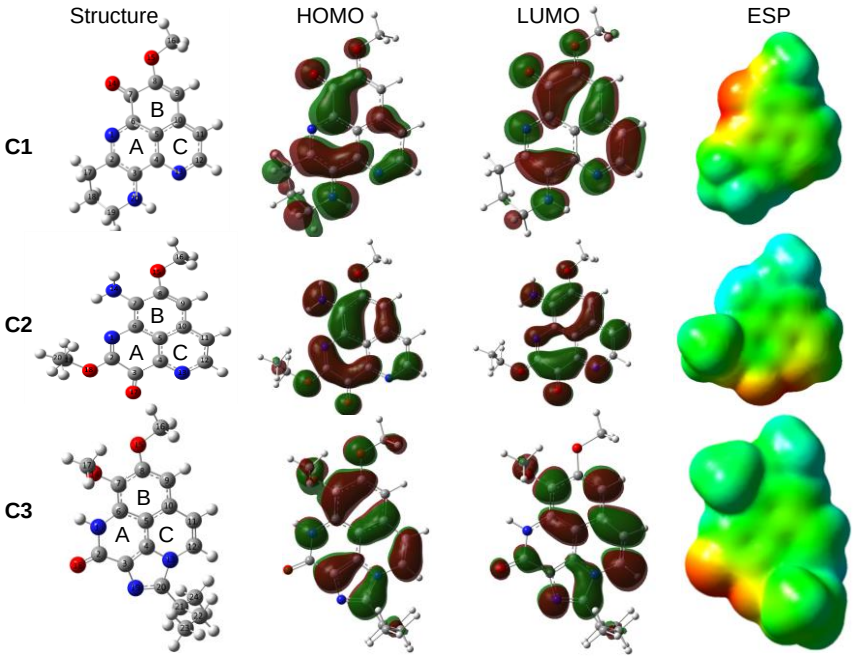

Figure 2. Optimized geometry, HOMO, LUMO, and ESP maps of **C1**–**C3** calculated in the gas phase at the M05-2X/6-311++G(d,p) level of theory (isovalue = 0.02).

3.3. Evaluation of antioxidant potential *via* intrinsic thermochemical parameters

Table 2 presented the intrinsic thermochemical parameters such as BDE, IP and PA which are examined *via* the HAT (**R1**), SET (**R2**) and PL (**R3**) mechanisms, respectively.

As can be seen in Table 2, the most favorable H donating positions for **C1** and **C3** are found at C–H bonds. For example, the **C1** exhibits the lowest BDE at C17 and C19 positions, being 85.5 and 85.7 kcal.mol^{-1}, respectively, whereas **C3** has the lowest BDE value at C21 position, *i.e.* 84.6 kcal.mol^{-1}. For **C2**, the easiest breaking-bond characterized by the lowest BDE value is located at N14 position (92.4 kcal.mol^{-1}). It is noteworthy that BDE values of **C1** and **C3** are much lower than that of the standard antioxidant Trolox in the gas phase (*i.e.* 91.1 kcal.mol^{-1}).[43] Consequently, the antioxidant potential of these aaptamines *via* HAT process can be classified in the following order: **C2** < Trolox < **C1** < **C3**. We observed a very slight change of BDE values in water for all compounds **C1-C3**. The only exception is obtained for **C1** at C19 position, with a BDE value in water lowering to 79.7 kcal.mol^{-1} *vs.* 85.7 kcal.mol^{-1} in gas phase. This result is not unexpected taken into account the neutral nature of the H atom species that is transferred.

The proton donating reaction from the aaptamines to free radical is characterized by the proton affinity (PA, eq.3); the lower the PA value, the better the antioxidant potential. As can be seen in Table 2, the lowest PA value of **C1** is 342.5 kcal.mol^{-1} (at C20 position), that of **C2** is 343.5 kcal.mol^{-1} (at N14 position) and the one of **C3** being

of 347.2 kcal.mol^{-1} (at N1 position). These PA values are quite similar to that of cembrene in the gas phase (*i.e.* 343.2 kcal.mol^{-1}). The proton donating ability of the three compounds in reaction with free radical according to the PL process is in the increasing order: **C3** < cembrene ≈ **C2** < **C1**. It is noteworthy that the PL is much preferred in water, for which the PA values are significantly reduced to a value of about 60 kcal.mol^{-1}. The result is totally in agreement with previous studies.[44]

Ionization potential (IP), characteristic for SET mechanism, is the minimum energy required to transfer an electron from the studied compound to free radical to form cationic species at ground state. The lower the IP value, the easier the electron transferring ability, thus, the antioxidant activity *via* SET mechanism will be higher. According to the results presented in Table 2, the adiabatic IP of **C1–C3** varied from 168 to 169 kcal.mol^{-1}, which is slightly higher than that of Trolox (*i.e.* 164.6 kcal.mol^{-1}) and lower than the one of cembrene (*i.e.* 171.9 kcal.mol^{-1}).[43] The antioxidant activities of the studied aaptamines following the SET mechanism increases in the order: Trolox < **C2** < **C1** < **C3** < cembrene. Similar to the proton transfer, the electron transfer is also favorable in water, with IP values reducing from 168−169 kcal.mol^{-1} in gas phase to 109−114 kcal.mol^{-1} in water, while remaining in the same order **C2** < **C1** < **C3**.

Overall, three aaptamines **C1–C3** are potential antioxidants. In the gas phase, the HAT mechanism can be responsible for the antioxidant properties of the molecules while in water the PL mechanism is particularly favorable.

Table 2: BDE, PA and adiabatic IP values (in kcal.mol^{-1}) of the **C1–C3** calculated in the gas phase at the M05-2X/6-311++G(d,p) level of theory. Corresponding values in water are given in parentheses.

C1				**C2**				**C3**			
Pos	**BDE**	**PA**	**IP**	**Pos**	**BDE**	**PA**	**IP**	**Pos**	**BDE**	**PA**	**IP**
C9	111.8	371.6	168.6 (110.0)	C9	113.9	366.7	168.3 (109.2)	C9	113.7	368.9	169.3 (114.0)
C11	114.3	374.4		C11	113.5	376.3		C11	114.9	371.3	
C12	106.2	383.6		C12	107.3	387.6		C12	114.4	360.6	
C16	97.1	367.1		C16	97.6	384.4		C16	96.5	384.2	
C17	85.5 (85.6)	366.4		C19	94.7	377.8		C17	97.3	389.3	
C18	98.9	390.7		C20	100.8			C21	84.6 (84.9)	366.3	
C19	85.7 (79.7)	361.7		N14	92.4 (91.6)	343.5 (59.6)		C22	95.6	396.0	
C20	93.2	342.5 (60.2)						C23	99.8	360.7	
								C24	99.0	390.4	
								N1	101.8	347.2 (59.7)	

3.4. HOO$^{\bullet}$ and HO$^{\bullet}$ free radical scavenging

The antioxidant potential of the studied aaptamines is investigated through the interactions with two representative free radicals, HOO$^{\bullet}$ and OH$^{\bullet}$ *via* four distinguished processes: hydrogen atom transfer (HAT), proton loss (PL), radical adduct formation (RAF), and single electron transfer (SET) mechanism (**R4** – **R7**). The $\Delta_r G^0$ of HAT, PL and RAF reactions between antioxidant and HOO$^{\bullet}$ and HO$^{\bullet}$ radicals are shown in Table 3 and Table 4, respectively. The reaction *via* SET mechanism is separately presented in Table 5.

As shown in the Table 3, in the gas phase, the Gibbs free energy values ($\Delta_r G^0$) for HAT reaction (**R4**) towards HOO$^{\bullet}$ are positive at all H-donating positions, ranging from 0.2 to 30.5 kcal.mol^{-1}. This result indicates that the potential for HOO$^{\bullet}$ removal *via* HAT mechanism of all three investigated compounds is not spontaneous and not favorable. Similarly, the proton transferring process (PL, **R5**) has positive $\Delta_r G^0$ at all of the positions; thus, the ability to remove HOO$^{\bullet}$ free radicals by PL process also is not favored in the gas phase. Concerning the RAF mechanism (**R6**), the $\Delta_r G^0$ found negative values at some specific positions. For example, the **C1** compound possesses highly negative $\Delta_r G^0$ of -13.0 and -12.6 kcal.mol^{-1} at C7 and C8 positions, respectively. For **C2**, HOO$^{\bullet}$ RAF process is highly negative at C2 position with $\Delta_r G^0$ being -9.8 kcal.mol^{-1}. Finally, for **C3**, the RAF reaction favorably occurs at C2 and C12 positions with $\Delta_r G^0$

value being -14.2 and -11.7 kcal.mol^{-1}, respectively. Thus, for the scavenging process towards HOO$^{\bullet}$ radical in the gas phase, the RAF is the only responsible mechanism. However, in water, HOO$^{\bullet}$ scavenging happened neither with the PL nor with the RAF mechanism; all the Gibbs free energies $\Delta_r G^0$ are obtained positive. Only with HAT mechanism, there are two positions, *i.e.* C19 of **C1** (-0.5 kcal.mol^{-1}) and C21 of **C3** (-0.4 kcal.mol^{-1}) give a spontaneous $\Delta_r G^0$.

Table 3: Gibbs free energy ($\Delta_r G^0$, kcal.mol^{-1}) of the HAT, PL, and RAF reaction of **C1**–**C3** towards HOO$^{\bullet}$ radical in the gas phase. Corresponding values calculated in water are given in parentheses for the most spontaneous reactions only. All calculation are performed at the M05-2X/6-311++G(d,p) level of theory.

HAT				**PL**				**RAF**			
Pos.	**C1**	**C2**	**C3**	**Pos.**	**C1**	**C2**	**C3**	**Pos.**	**C1**	**C2**	**C3**
C9	27.3	29.5	29.2	C9	219.8	214.9	217.0	C2	-1.0	-9.8 (5.2)	-
C11	29.8	29.0	30.5	C11	222.5	224.5	219.4	C3	-7.8	10.3	7.9
C12	21.7	22.8	29.9	C12	231.8	235.7	208.7	C4	14.4	2.4	2.6
C16	12.7	13.1	12.0	C16	224.3	232.5	232.3	C5	19.8	19.6	11.0
C17	1.0 (0.4)		12.8	C17	214.5		237.5	C6	-3.6	0.1	9.6
C18	14.4			C18	238.9			C7	-	-5.6	-7.4
C19	1.2 (-5.0)	10.2 (9.1)		C19	209.9	225.9		C8	-12.6 6.5	-1.5	3.7
C20	8.7	16.4		C20	190.6 (77.3)			C9	-6.1	7.0	-0.3
N14		7.9 (7.1)		N14		191.7 (77.5)		C10	8.3	16.5	9.8
N1			17.4	N1			195.3 (76.8)	C11	-4.0	-4.3	-1.4
C21			0.2 (-0.4)	C21			214.4	C12	0.4	3.4	-11.7 (3.0)
C22			11.1	C22			244.1				
C23			15.4	C23			208.9				
C24			14.5	C24			239.0				

Regarding to the OH$^{\bullet}$ scavenging activities (Table 3), the negative $\Delta_r G^0$ values are obtained at all positions of three studied compounds for both the HAT and RAF processes. This proves that **C1**-**C3** have high scavenging potential towards OH$^{\bullet}$ radical *via* HAT and RAF processes. The most active compound *via* HAT mechanism is awarded for **C1** (C17 position) and **C3** (C21 position), with the $\Delta_r G^0$ of -30.7 and -31.6 kcal.mol^{-1}, respectively. The lowest $\Delta_r G^0$ values for RAF mechanism are obtained for **C1** (C8 position) and **C2** (C2 position) compounds with the values in the gas phase of -41.6 and -39.3 kcal.mol^{-1}, respectively. For the proton transfer process, the positive value of $\Delta_r G^0$ is observed at all the positions for all aaptamines. This result is reasonable because the gas phase is not a favorable medium for the charge transferring process like the proton transfer. In general, the RAF towards OH$^{\bullet}$ is more favorable than the HAT and PL. For example, **C1** has the lowest $\Delta_r G^0$(HAT) being -30.7 kcal.mol^{-1}, whereas it has the lowest $\Delta_r G^0$(RAF) being -41.6 kcal.mol^{-1} and $\Delta_r G^0$(PL) being 407.9 kcal.mol^{-1}. In contrast, in water, the HAT is more competitive than the RAF. For example, the lowest $\Delta_r G^0$(HAT) of **C1** is lowered to -38.9 kcal.mol^{-1} at C19, while the lowest $\Delta_r G^0$(RAF) is obtained with **C3** with -24.6 kcal.mol^{-1} at C18 position. On the other hand, the PL process is always not spontaneous and not favorable.

Moreover, as can be seen in the Table 5, Gibbs free energy of the SET reactions (**R7**) are not favorable in our conditions with the $\Delta_r G^0$ value in the gas phase varying around 145 kcal.mol^{-1} for HOO$^{\bullet}$ radical and 130 kcal.mol^{-1} for HO$^{\bullet}$ radical. Although in water, the $\Delta_r G^0$ have been significantly decreased (15–41 kcal.mol^{-1}), the electron transfer is obviously not favorable.

Table 4: Gibbs free energy ($\Delta_r G^0$, kcal.mol^{-1}) of the HAT, PL, and RAF reaction of **C1**–**C3** towards HO$^\bullet$ radical in the gas phase. Corresponding values calculated in water are only given (in parentheses) for the most spontaneous reactions. All calculation are performed at the M05-2X/6-311++G(d,p) level of theory.

HAT				PL				RAF			
Pos.	**C1**	**C2**	**C3**	**Pos.**	**C1**	**C2**	**C3**	**Pos.**	**C1**	**C2**	**C3**
C9	-4.4	-2.3	-2.6	C9	437.0	432.1	434.3	C2		-39.3 (-23.6)	-
C11	-1.9	-2.7	-1.3	C11	439.8	441.7	436.6	C3	-33.0	-16.3	-7.9
C12	-10.0	-8.9	-1.9	C12	449.0	453.0	425.9	C4	-9.8	-21.7	-10.4
C16	-19.1	-18.6	-19.7	C16	441.5	449.7	449.5	C5	-4.2	-3.3	-2.5
C17	-30.7 (-33.6)		-18.9	C17	431.8		454.7	C6	-28.1	-23.2	-4.5
C18	-17.3			C18	456.1			C7	-17.8	-32.1	-26.7 (-24.6)
C19	-30.5 (-38.9)	-21.6 (-24.8)		C19	427.1	443.1		C8	-41.6 (-21.6)	-27.7	-16.1
C20	-23.0	-15.4		C20	407.9 (79.7)			C9	-31.6	-32.2	-15
N14		-23.8 (-26.8)		N14		408.9 (80.0)		C10	-15.0	-5.7	-2.1
N1			-14.4	N1			412.5 (79.2)	C11	-30.7	-30.7	-16.6
C21			-31.6 (-34.4)	C21			431.7	C12	-24.0	-20.4	-26.6 (-24.2)
C22			-20.6	C22			461.3				
C23			-16.4	C23			426.1				
C24			-17.3	C24			456.3				

Overall, the radical scavenging activities of the studied compounds favorably occur *via* RAF mechanism in the gas phase while in water it more likely occurs *via* HAT mechanism. The HO$^\bullet$ radical scavenging is much more favorable than the reaction with HOO$^\bullet$. Finally, the antioxidant potential *via* HAT process of the three studied compounds is classified in the increasing trend: **C2** < **C3** ≈ **C1**. For RAF mechanism, **C1** and **C2** are potent in gas phase while the **C3** is more effective in water.

Table 5: Gibbs free energy ($\Delta_r G^0$, kcal.mol^{-1}) of SET reaction towards OOH$^\bullet$/OH$^\bullet$ free radical

	OOH$^\bullet$			**OH$^\bullet$**		
	C1	**C2**	**C3**	**C1**	**C2**	**C3**
Gas	145.1	144.8	145.5	129.7	129.5	130.2
Wat.	37.4	37.2	41.1	15.3	15.2	19.0

3.5. Kinetics

The kinetics of the possible reactions were studied with the neutral forms of **C1-C3** in gas phase and water, for the OOH$^\bullet$ scavenging. The Gibbs free energy of activation ($\Delta G^{\ddagger}$) and transition state theory (TST) rate constant (k_{TST}) for all reactions were systematically calculated in the gas phase and in water at the M05-2X/6-311++G(d,p) level of theory. Gibbs free energy of activation and TST rate constants obtained in the gas phase are presented in **Table 6**.

For HAT reaction, because **C2** have all high positive Gibbs free energy of the reaction for all the H donating positions, we did not apply the kinetic calculation for this compound. Indeed, the compounds **C1** and **C3** display the activation Gibbs free energy of 16.8 and 19.8 kcal/mol, respectively. Similar rate constants are also obtained for two compounds **C1** and **C3** (~ 10^{-19} cm^3.molecule^{-1}.s^{-1}), which is much larger than the one of a standard antioxidant such as ascorbic acid (~ 10^{-15} cm^3.molecule^{-1}.s^{-1}). For the RAF reaction, the lowest activation Gibbs free energy (14.0 kcal/mol) and the highest rate constant (3.80 × 10^{-18} cm^3.molecule^{-1}.s^{-1}) are obtained at the position C2 of aaptamine **C2**, indicate the most favorable reaction. At the second place, the **C1**

and ascorbic acid, are found with similar activation Gibbs free energy of about 14.8-15.0 kcal/mol and rate constants of $3.4 - 3.6 \times 10^{-19}$ $cm^3.molecule^{-1}.s^{-1}$. In contrary, the SET reaction is found with very high activation energy of about 400 kcal/mol and near-zero rate constants.

Table 6: Gibbs free energy of activation ($\Delta G^{\ddagger}$, in $kcal.mol^{-1}$) at standard concentration (1M) and TST rate constant (k_{TST}, in $cm^3.molecule^{-1}.s^{-1}$) including the Eckart tunneling correction at 298.15 K calculated in the gas phase for HAT, RAF and SET reactions of **C1**–**C3** towards HOO• radical. Calculations are performed at the M05-2X/6-311++G(d,p) level of theory.

Reaction	$\Delta G^{\ddagger,1M}$, kcal.mol^{-1}	$k_{TST}^{,298.15K}$, cm^3.molecule^{-1} · s^{-1}
HAT		
C1@C19H + HOO•	16.8	9.10×10^{-19}
C3@C21H + HOO•	19.8	2.30×10^{-19}
Ascorbic + HOO•	9.2	3.10×10^{-15}
RAF		
C1@C8 + HOO•	14.8	3.40×10^{-19}
C2@C2 + HOO•	14.0	3.80×10^{-18}
C3@C12 + HOO•	15.6	7.60×10^{-21}
Ascorbic + HOO•	15.0	3.60×10^{-19}
SET		
C1 + HOO•	420.9	4.30×10^{-295}
C2 + HOO•	378.7	3.93×10^{-264}
C3 + HOO	401.3	1.05×10^{-280}

For the reactions in water, kinetics data including the Gibbs free energy of activation $\Delta G^{\ddagger}$, the diffusion rate constants k_D, thermal rate constant k_T, Eckart-tunneling-corrected rate constants $k_{eck,}$ diffusion-corrected rate constants k_{app}, and the branching ratio Γ for each reaction HAT, RAF and SET are resumed in **Table 7**.

For HAT reaction at the C19H position of **C1**, it happens to be a barrierless reaction, with negative Gibbs free energy of activation (-0.87 kcal/mol). Moreover, the rate constant obtained at this position is of 7.13×10^6 M^{-1} s^{-1}. This is also the dominant reaction with for **C1**. In contrary, the **C3** requires 5.17 kcal/mol of Gibbs free energy of activation and appears with a rate constant of only 3.84×10^3 M^{-1} s^{-1}. For RAF reaction, the reaction barriers ($\Delta G^{\ddagger}$) are found 5.6, 7.2 and 7.5 kcal/mol for **C1**, **C2**, **C3**, respectively. As can be seen in the **Table 6**, the diffusion rate constants k_D of RAF are dominant, with values of about 10^9 M^{-1} s^{-1}, while the thermal rate constants are much smaller (~10^5 M^{-1} s^{-1}). The fastest reaction is observed with **C2** at the C2 position (k_{app} = 1.40×10^5 M^{-1} s^{-1}). Similar as in the gas phase, the SET reaction of all three compounds requires very high activation Gibbs free energy (45–53 kcal/mol) and occurred at extremely small rate (10^{-25}–10^{-20} M^{-1} s^{-1}). Overall, we observed a competition of the HAT and RAF reaction for the HOO• scavenging. For **C1**, the HAT reaction is dominant, while the HOO• scavenging *via* RAF is more favored with **C2** and **C3**.

Table 7: Gibbs free energy of activation ($\Delta G^{\ddagger}$, kcal mol^{-1}), diffusion rate constant (k_D, M^{-1} s^{-1}), TST thermal rate constant (k_T, M^{-1} s^{-1}), Eckart-tunneling-corrected rate constants (k_{eck}, M^{-1} s^{-1}) and diffusion-corrected apparent rate constants (k_{app}, M^{-1} s^{-1}) calculated at 298 K for the HAT, RAF and SET mechanism with HOO• radical in water.

Reaction path	$\Delta G^{\ddagger,1M}$, kcal.mol^{-1}	k_D, M^{-1} s^{-1}	k_T, M^{-1} s^{-1}	k_{eck}, M^{-1} s^{-1}	k_{app}, M^{-1} s^{-1}	Γ, %
HAT						
C1@C19H + HOO•	-0.87	1.40×10^9	7.17×10^6	3.22×10^{-15}	7.13×10^6	96
C3@C21H + HOO•	5.17	1.27×10^9	3.84×10^3	3.22×10^{-16}	3.84×10^3	1
RAF						
C1@C8 + HOO•	7.2	2.10×10^9	3.00×10^7	2.80×10^5	2.80×10^5	4
C2@C2 + HOO•	5.6	2.20×10^9	4.20×10^8	1.40×10^5	1.40×10^5	100
C3@C12 + HOO•	7.5	2.00×10^9	1.90×10^7	2.90×10^5	2.90×10^5	99
SET						
C1 + HOO•	47.10	8.22×10^9	4.56×10^{-21}	-	4.56×10^{-21}	0
C2 + HOO•	45.91	8.26×10^9	3.35×10^{-20}	-	3.35×10^{-20}	0
C3 + HOO•	53.19	8.47×10^9	1.55×10^{-25}	-	1.55×10^{-25}	0

3.6. UV radiation absorption properties

The vertical excitation of the molecules **C1-C3** is studied with TD-DFT using different functionals such as B3LYP, B98, M06, PBE0, CAM-B3LYP and M05-2X as previously recommended for accuracy. [39] In order to compare with experimental data reported in MeOH,[4] all calculation is performed in MeOH using the implicit model IEF-PCM. The lowest absorption wavelength of each compound calculated by six above-mentioned functionals is presented in the Table 8 in comparison with the measured data.

As can be seen in Table 8, among the different methods, a fairly consistent result in comparison with the experimental data is obtained with CAM-B3LYP and M05-2X functional. For example, the lowest absorption of **C1** calculated in MeOH by M05-2X is found at 423 nm while the experimental value was reported at 398 nm in the same solvent (25 nm deviation). Similar deviation of about 30 nm was obtained for **C2**. However, a much higher deviation is observed with **C3**, for which a shorter wavelength of 292 nm is absorbed *vs.* 350 nm in measurement. The other methods, which comprise a portion of 20–30 % HF in exchange correlation give much less-comparative absorption. For example, the B3LYP functional (20 % HF) provides much higher absorption wavelengths, *i.e*. 471, 482 and 332 nm for **C1-C3**, respectively. As discussed in the literature, the main drawback of TD-DFT consists of the underestimation of the vertical excited energy, for which a significant error up to 0.4 eV can be found.[45] However, for comparative purpose, the TD-DFT results in general can still provide a benefit when it treats with the same kind of molecules.

Table 8. Lowest absorption wavelength (nm) of **C1**–**C3** calculated by TD-DFT with different methods of various % HF in exchange correlation.

Method	%HF	Absorption / nm		
		C1	C2	C3
B3LYP	20	471	482	332
B98	22	465	476	327
M06	27	461	472	329
PBE0	25	459	470	322
CAM-B3LYP*	19/65	427	439	298
M05-2X	56	423	435	292
Exp. (ref.4)		398	402	350

*19 % HF at short-range and 65 % HF at long-range

The vertical excited energy of some lowest excitations calculated by TD/M05-2X/6-311++G(d,p) as well as the oscillator strength and the nature of the corresponding electronic transition are presented in Table 9. Vertical excitations of **C1**, **C2**, and **C3** is found at 2.93, 2.87 and 4.24 eV, respectively. In all cases, we observed mainly the contribution of the HOMO to LUMO transition for the lowest lying excitation of **C1-C3**. This contribution varies from 96 % for **C1**, 97 % for **C2** and 86 % for **C3**. As predicted in the electronic properties part, the HOMO and LUMO of three compounds involved mostly the rings of aaptamine derivatives, then all the lowest absorption is characterized as π-π* transition.

Table 9. Vertical excited energies (eV), absorption wavelength (nm), oscillator strength *f* and the corresponding electronic transition of some lowest excited states of **C1-C3** calculated by TD-DFT at M05-2X/6-311++G(d,p) in MeOH.

Cp	ES	E/eV	λ/nm	*f*	Transition	%
C1	S1	2.93	423	0.3553	H → L	96
	S3	3.60	345	0.1614	H-1 → L	91
	S7	4.84	257	0.4625	H-2 → L H → L+1	47 43
	S8	5.33	233	0.1603	H → L+2	92
		5.72	212	0.0277	H-1 → L+1 H → L+3	62 24
C2	S1	2.87	435	0.2938	H → L	97
	S3	3.78	328	0.1196	H-1 → L H-3 → L	86 6
	S6	5.01	248	0.6778	H → L+1 H-1 → L H-3 → L	77 8 8
	S8	5.24	237	0.1734	H → L+2 H-3 → L	83 8
C3	S1	4.24	292	0.1447	H → L H-1 → L+1	86 8
	S3	4.90	253	0.5688	H → L+1 H → L+2 H-1 →L H-1 → L+2	45 21 15 9
	S4	5.22	238	0.1517	H-1 → L+2 H-1 →L H → L+2 H → L+1	72 13 6 5
	S5	5.46	227	0.9586	H → L+2 H-1 → L H-1 → L+1 H-1 → L+2 H → L+1	55 15 8 8 7
	S7	5.71	217	0.2460	H-1 → L+2 H-2 → L H → L+2 H → L+6	49 18 15 5

Finally, the Figure 3 displayed the energy gap and energy level of the frontier molecular orbitals that participated to the lowest electronic transition of the **C1**–**C3**. One can easily notice that: *(i)* there is a much lower gap (4.9 eV) for **C1** and **C2** in comparison with 6.5 eV gap in case of **C3**, and

(ii) possessing the same energy level for HOMO, the energy level of LUMO of **C1** and **C2** is much lower than that of **C3**. All results indicate that the **C1** and **C2** can be easily excited within the visible (blue) and UV range while the **C3** are effective UV absorption agent. The results suggest the use of aaptamines **C1–C3** as photo-protective agents.

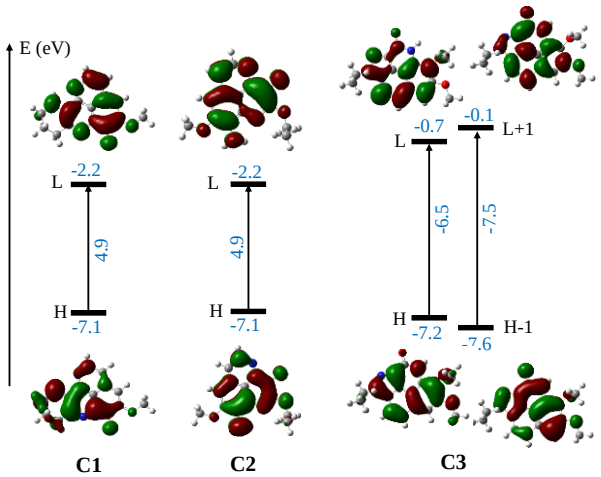

Figure 3. The energy gap and energy levels of the frontier molecular orbitals which participated to the lowest electronic transition of **C1**–**C3**. The result is obtained with DFT/M05-2X/6-311++G(d,p) in MeOH (IEF-PCM).

4. CONCLUSIONS

The antioxidant activities of three aaptamines (**C1, C2** and **C3**) extracted from sponges was investigated in the gas phase and water using DFT method according to four mechanisms: HAT, SET, PL and RAF. All of these investigated compounds exhibited the best antioxidant activity *via* RAF mechanism, for which antioxidant potential is classified in the increasing order **C2** < **C1** < **C3** for $HOO^{\bullet}$ and **C3** < **C2** < **C1** for $HO^{\bullet}$ free radical scavenging activity. Furthermore, HAT mechanism is elucidated as the second competitive mechanism, in particularly for $HO^{\bullet}$ quenching and in water. Thermodynamically, the antioxidant activities *via* four studied processes are in the decreasing order as follows: RAF > HAT > SET > PL (gas) and HAT > RAF > SET > PL (water). Kinetic calculation show that the HAT mechanism is the most favorable path for $HOO^{\bullet}$ scavenging in water with **C1** while the RAF is more competitive with **C2** and **C3**. Second, all compounds, particularly the **C3**, are effective in the UV absorption. Within the range of our study, the M05-2X level provides the best performance for calculation of vertical excited energy using TD-DFT. These results promote aaptamine derivatives as natural antioxidant and anti-UV agents for the use in human healthcare such as in pharmaceutics and cosmetics.

Acknowledgments. This research is funded by Vietnam National Foundation for Science and Technology Development (NAFOSTED) under grant number 103.01-2019.380. The authors are grateful for the help in kinetic calculation from Dr. Thi Chinh Ngo and Mr. Dinh Hieu Truong (Duy Tan University).

Conflict of interest. The authors declare no conflict of interest.

REFERENCES

1. Shaari, K.; Ling, K. C.; Rashid, Z. M.; Jean, T. P.; Abas, F.; Raof, S. M.; Zainal, Z.; Lajis, N. H.; Mohamad, H.; Ali, A. M., Cytotoxic Aaptamines from Malaysian Aaptos aaptos. *Marine Drugs* **2009,** *7*, 1-8.

2. Shubina, L. K.; Kalinovsky, A. I.; Fedorov, S. N.; Radchenko, O. S.; Denisenko, V. A.; Dmitrenok, P. S.; Dyshlovoy, S. A.; Krasokhin, V. B.; Stonik, V. A., Aaptamine Alkaloids from the Vietnamese Sponge Aaptos sp. *Nat. Prod. Commun.* **2009,** *4* (8), 1085-1088.

3. Pham, C. D.; Hartmann, R.; Muller, W. E.; de Voogd, N.; Lai, D.; Proksch, P., Aaptamine derivatives from the Indonesian sponge Aaptos suberitoides. *J. Nat. Prod.* **2013,** *76* (1), 103-106.

4. Nakamura, H.; Kobayashi, J.; Ohizumi, Y.; Hirata, Y., Isolation and structure of aaptamine a novel heteroaromatic substance possessing a-blocking activity from the sea sponge aaptos aaptos. *Tetrahedron Letters* **1982,** *23* (52), 5555-5558.

5. Yu, H.-B.; Yang, F.; Sun, F.; Li, J.; Jiao, W.-H.; Gan, J.-H.; Hu, W.-Z.; Lin, H.-W., Aaptamine Derivatives with Antifungal and Anti-HIV-1
Activities from the South China Sea Sponge Aaptos aaptos. *Marine Drugs* **2014,** *12*, 6003-6013.

6. Bowling, J. J.; Pennaka, H. K.; Ivey, K.; Wahyuono, S.; Kelly, M.; Schinazi, R. F.; Valeriote, F. A.; Graves, D. E.; Hamann, M. T., Antiviral and anticancer optimization studies of the DNA-binding marine natural product aaptamine. *Chem. Biol. Drug Des.* **2008,** *71* (3), 205-215.

7. Rajivgandhi, G.; kumar, S. N.; Ramachandran, G.; Manoharan, N., Marine sponge alkaloid aaptamine enhances the anti-bacterial and anti-cancer activity against ESBL producing Gram negative bacteria and HepG 2 human liver carcinoma cells. *Biocat. Agri. Biotech.* **2019,** *17*, 628-637.
8. Yu, H. B.; Yang, F.; Sun, F.; Ma, G. Y.; Gan, J. H.; Hu, W. Z.; Han, B. N.; Jiao, W. H.; Lin, H. W., Cytotoxic aaptamine derivatives from the South China Sea sponge Aaptos aaptos. *J. Nat. Prod.* **2014,** *77* (9), 2124-2129.
9. (a) Dyshlovoy, S. A.; Fedorov, S. N.; Shubina, L. K.; Kuzmich, A. S.; Bokemeyer, C.; Keller-von Amsberg, G.; Honecker, F., Aaptamines from the marine sponge Aaptos sp. display anticancer activities in human cancer cell lines and modulate AP-1-, NF-kappaB-, and p53-dependent transcriptional activity in mouse JB6 Cl41 cells. *Biomed. Res. Int.* **2014,** *2014*, 469309; (b) Dyshlovoy, S. A.; Venz, S.; Shubina, L. K.; Fedorov, S. N.; Walther, R.; Jacobsen, C.; Stonik, V. A.; Bokemeyer, C.; Balabanov, S.; Honecker, F., Activity of aaptamine and two derivatives, demethyloxyaaptamine and isoaaptamine, in cisplatin-resistant germ cell cancer. *J. Proteomics* **2014,** *96*, 223-239.
10. Hamada, T.; Matsumoto, Y.; Phan, C.-S.; Kamada, T.; Onitsuka, S.; Okamura, H.; Iwagawa, T.; Arima, N.; Tani, F.; Vairappan, C. S., Aaptamine-Related Alkaloid from the Marine Sponge Aaptos aaptos. *Nat. Prod. Commun.* **2019,** *14* (9), 1-3.
11. Takamatsu, S.; Hodges, T. W.; Rajbhandari, I.; Gerwick, W. H.; Hamann, M. T.; Nagle, D. G., Marine Natural Products as Novel Antioxidant Prototypes. *J. Nat. Prod.* **2003,** *66*, 605-608.
12. Krutmann, J.; Bouloc, A.; Sore, G.; Bernard, B. A.; Passeron, T., The skin aging exposome. *J. Dermatol. Sci.* **2017,** *85* (3), 152-161.
13. Cadet, J.; Douki, T.; Ravanat, J. L.; Di Mascio, P., Sensitized formation of oxidatively generated damage to cellular DNA by UVA radiation. *Photochem. Photobiol. Sci.* **2009,** *8* (7), 903-911.
14. Fourtanier, A.; Moyal, D.; Seite, S., UVA filters in sun-protection products: regulatory and biological aspects. *Photochem. Photobiol. Sci.* **2012,** *11* (1), 81-89.
15. Dunaway, S.; Odin, R.; Zhou, L.; Ji, L.; Zhang, Y.; Kadekaro, A. L., Natural Antioxidants: Multiple Mechanisms to Protect Skin From Solar Radiation. *Front. Pharmacol.* **2018,** *9*, 392.
16. Latha, M. S.; Martis, J.; V, S.; Shinde, R. S.; Bangera, S.; Krishnankutty, B.; Bellary, S.; Varughese, S.; Rao, P.; Kumar, B. R. N., Sunscreening Agents: A review. *J. Clin. Aesth. Dermatol.* **2013,** *6* (1), 16-26.
17. Stevanato, R.; Bertelle, M.; Fabris, S., Photoprotective characteristics of natural antioxidant polyphenols. *Regul. Toxicol. Pharmacol.* **2014,** *69* (1), 71-77.
18. Freitas, J. V.; Praca, F. S.; Bentley, M. V.; Gaspar, L. R., Trans-resveratrol and beta-carotene from sunscreens penetrate viable skin layers and reduce cutaneous penetration of UV-filters. *Int. J. Pharm.* **2015,** *484* (1-2), 131-137.
19. Peres, D. D.; Sarruf, F. D.; de Oliveira, C. A.; Velasco, M. V. R.; Baby, A. R., Ferulic acid photoprotective properties in association with UV filters: multifunctional sunscreen with improved SPF and UVA-PF. *J. Photochem. Photobiol. B* **2018,** *185*, 46-49.
20. Scalia, S.; Mezzena, M., Photostabilization Effect of Quercetin on the UV Filter Combination, Butyl Methoxydibenzoylmethane–Octyl Methoxycinnamate. *Photochem. Photobiol.* **2010,** *86*, 273–278.
21. Masaki, H., Role of antioxidants in the skin: anti-aging effects. *J. Dermatol. Sci.* **2010,** *58* (2), 85-90.
22. Rioux, B.; Peyrot, C.; Mention, M. M.; Brunissen, F.; Allais, F., Sustainable Synthesis of p-Hydroxycinnamic Diacids through Proline-Mediated Knoevenagel Condensation in Ethanol: An Access to Potent Phenolic UV Filters and Radical Scavengers. *Antioxidants* **2020,** *9* (4), 331.
23. Dao, D. Q.; Phan, T. T. T.; Nguyen, T. L. A.; Trinh, P. T. H.; Tran, T. T. V.; Lee, J. S.; Shin, H. J.; Choi, B. K., Insight into Antioxidant and Photoprotective Properties of Natural Compounds from Marine Fungus. *J. Chem. Inf. Model.* **2020,** *60* (3), 1329-1351.
24. Gaussian 16, A., M. J. Frisch, G. W. Trucks, H. B. Schlegel, G. E. Scuseria, M. A.

Robb, J. R. Cheeseman, G. Scalmani, V. Barone, G. A. Petersson, H. Nakatsuji, X. Li, M. Caricato, A. Marenich, J. Bloino, B. G. Janesko, R. Gomperts, B. Mennucci, H. P. Hratchian, J. V. Ortiz, A. F. Izmaylov, J. L. Sonnenberg, D. Williams-Young, F. Ding, F. Lipparini, F. Egidi, J. Goings, B. Peng, A. Petrone, T. Henderson, D. Ranasinghe, V. G. Zakrzewski, J. Gao, N. Rega, G. Zheng, W. Liang, M. Hada, M. Ehara, K. Toyota, R. Fukuda, J. Hasegawa, M. Ishida, T. Nakajima, Y. Honda, O. Kitao, H. Nakai, T. Vreven, K. Throssell, J. A. Montgomery, Jr., J. E. Peralta, F. Ogliaro, M. Bearpark, J. J. Heyd, E. Brothers, K. N. Kudin, V. N. Staroverov, T. Keith, R. Kobayashi, J. Normand, K. Raghavachari, A. Rendell, J. C. Burant, S. S. Iyengar, J. Tomasi, M. Cossi, J. M. Millam, M. Klene, C. Adamo, R. Cammi, J. W. Ochterski, R. L. Martin, K. Morokuma, O. Farkas, J. B. Foresman, and D. J. Fox, Gaussian, Inc., Wallingford CT, 2016.

25. Zhao, Y.; Schultz, N. E.; Truhlar, D. G., Design of Density Functionals by Combining the Method of Constraint Satisfaction with Parametrization for Thermochemistry, Thermochemical Kinetics, and Noncovalent Interactions. *J. Chem. Theo. Comput.* **2006,** *2* (2), 364-382.

26. Galano, A.; Alvarez-Idaboy, J. R., A computational methodology for accurate predictions of rate constants in solution: application to the assessment of primary antioxidant activity. *J. Comput. Chem.* **2013,** *34* (28), 2430-45.

27. Galano, A.; Alvarez-Idaboy, J. R., Kinetics of Radical-Molecule Reactions in Aqueous Solution: A Benchmark Study of the Performance of Density Functional Methods. *J. Comput. Chem.* **2014,** *35*.

28. Bartmess, J. E., Thermodynamics of the Electron and the Proton. *J. Phys. Chem.* **1994,** *98*, 6420-6424.

29. Marković, Z.; Tošović, J.; Milenković, D.; Marković, S., Revisiting the solvation enthalpies and free energies of the proton and electron in various solvents. *Comp. Theo. Chem.* **2016,** *1077*, 11-17.

30. Dzib, E.; Cabellos, J. L.; Ortíz-Chi, F.; Pan, S.; Galano, A.; Merino, G., Eyringpy: A program for computing rate constants in the gas phase and in solution. *Int. J. Quant. Chem.* **2018,** *119* (2), e25686.

31. Okuno, Y., Theoretical investigation of the mechanism of the Baeyer - Villiger reaction in nonpolar solvents. *Chem. Eur. J.* **1997,** *3* (2), 212-218.

32. Benson, S. W., *The Foundations of Chemical Kinetics*. 1982.

33. Marcus, R. A., Chemical and Electrochemical Electron-transfer Theory. *Annu. Rev. Phys. Chem.* **1964,** *15*, 155-196.

34. Collins, F. C.; Kimball, G. E., Diffusion-controlled reaction rates. **1949**, 425-437.

35. Smoluchowski, M. v., Versuch einer mathematischen Theorie der Koagulationskinetik kolloider Lösungen. *Z. Phys. Chem* **1918,** *92*, 129-168.

36. (a) Einstein, A., Über die von der molekularkinetischen Theorie der Wärme geforderte Bewegung von in ruhenden Flüssigkeiten suspendierten Teilchen. *Ann. Phys.* **1905,** *332* (8), 549-560; (b) Stockes, G. G., Mathematical and Physical Papers. Cambridge: The University Press: New York: The Macmillan Co., , 1905; Vol. V.

37. Jang, Y. H.; Sowers, L. C.; Cagin, T.; III, W. A. G., First Principles Calculation of pKa Values for 5-Substituted Uracils. *J. Phys. Chem. A* **2001,** *105*, 274-280.

38. Shields, G. C.; Seybold, P. G., *Computational Approaches for the Prediction of pKa Values*. CRC Press, Taylor & Francis Group: 2014.

39. Jacquemin, D.; Mennucci, B.; Adamo, C., Excited-state calculations with TD-DFT: from benchmarks to simulations in complex environments. *Phys. Chem.Chem. Phys.* **2011,** *13* (38), 16987-16998.

40. Tomasi, J.; Mennucci, B.; Cancès, E., The IEF version of the PCM solvation method: an overview of a new method addressed to study molecular solutes at the QM ab initio level. *Journal of Molecular Structure: THEOCHEM* **1999,** *464* (1), 211-226.

41. Bordwell, F. G.; Algrim, D.; Vanier, N. R., Acidities of Anilines and Toluenes. *J. Org. Chem.* **1977,** *42* (10), 1817-1819.

42. Bordwell, F. G.; Algrim, D. J., Acidities of Anilines in Dimethyl Sulfoxide Solution. *J. Am. Chem. Soc.* **1988,** *110*, 2964-2968.

43. Farmanzadeh, D.; Najafi, M., Novel Trolox derivatives as antioxidant: A DFT

investigation. *J. Serbian Chem. Soc.* **2016,** *81* (3), 277-290.
44. Ngo, T. C.; Nguyen, T. H.; Dao, D. Q., Radical Scavenging Activity of Natural-Based Cassaine Diterpenoid Amides and Amines. *J. Chem. Inf. Model.* **2019,** *59* (2), 766-776.
45. Dreuw, A.; Head-Gordon, M., Failure of Time-Dependent Density Functional Theory for Long-Range Charge-Transfer Excited States: The Zincbacteriochlorin−Bacteriochlorin and Bacteriochlorophyll−Spheroidene Complexes. *Journal of the American Chemical Society* **2004,** *126* (12), 4007-4016.

Corresponding author:

Thi Le Anh Nguyen,
Institute of Research and Development,
Faculty of Natural Sciences,
Duy Tan University, 03 Quang Trung, Da Nang, 550000, Vietnam.
Email: nguyenthileanh@duytan.edu.vn